JTTEE5 6:199-204


# Graded Plasma Spraying of Premixed Metal-Ceramic Powders on Metallic Substrates

*C.R.C. Lima and R.-E. Trevisan*

**The mismatch between the thermal expansion coefficients of ceramics and metals and the differential stresses it causes at the interface create problems in metal to ceramic joining. Research has been conducted to solve this problem in thermal barrier coating technology. Previous studies have considered metal-ceramic multilayers or graded-coatings, which include a metallic bond coat. In this study, a graded plasma-sprayed metal-ceramic coating is developed using the deposition of premixed metal and ceramic powders without the conventional metallic bond coat. Influences of thickness variations, number, and composition of the layers are investigated. Coatings are prepared by atmospheric plasma-spraying on Inconel 718 superalloy substrates. Ni-Cr-Al and $ZrO_2$-8% $Y_2O_3$ powders are used for plasma spraying. Adhesive and cohesive strength of the coatings are determined. The concentration profile of the elements is determined by x-ray energy-dispersive analysis. The microstructure and morphology of the coatings are investigated by optical and scanning electron microscopy (SEM). Results show that the mixed metal-ceramic coating obtained with the deposition of premixed powders is homogeneous. The morphology and microstructure of the coatings are considered satisfactory.**

**Keywords** coating, composition gradient, graded coating, metal-ceramic, plasma spraying, thermal barrier, zirconia

## 1. Introduction

THERMAL EXPANSION coefficient mismatch between different materials, which may lead to excessive stresses at the interface (Ref 1), is the main cause of problems in metal-ceramic joining. This is also a common problem for ceramic coatings applied on metals, such as thermal barrier coating (TBC) technology. Thermal barrier coatings are typically composed of a metallic bond coat layer and an insulating ceramic coating layer, termed a duplex system (Ref 2). The metallic bond coating is usually a MCrAlY alloy, where M stands for iron, indium, cobalt, or combinations of these elements. The ceramic coating is usually zirconia, partially stabilized with 8 wt% yttria. Both the metallic and ceramic coating layers are applied using the plasma-spray process. The insulating capacity of a TBC system is incontestable. However, the durability and mechanical properties of a TBC may strongly vary with several factors, including process conditions, operating conditions, and materials.

A widely discussed reason for the spallation of plasma-spray TBCs is the residual stress in the system consisting of ceramic top coating, metallic bond coat, and metallic substrate. Residual stresses are caused by mismatch of the thermal expansion coefficients of the materials and by oxidation of the bond coat (Ref 3). Dorfman et al. (Ref 4), in a study of TBCs for diesel engines, demonstrated improvement of the residual stress by controlling spray temperature and by using a graded coating concept. The proposed system consists of a metal bond coat, two cermet (metal-zirconia) intermediate coating layers, and a ceramic top coat (zirconia). The total thickness of this coating can reach 2.54 mm (0.100 in.). Tsai and Tsai (Ref 5) describe operating procedures for laser glazing of plasma-sprayed yttria-stabilized zirconia coatings to improve the coating performance, mainly through control of the bond coat oxidation resistance by reducing the ceramic top coat porosity. Microhardness is increased from about 550 Vickers hardness (HV) for the as-sprayed layer to 1550 HV for the as-glazed layer. Microcracks are formed in the columnar structure and improve the coating performance by optimizing the residual stresses.

Demasi-Macin and Gupta (Ref 6) describe thermal barrier graded coatings for turbine abradable seal systems. These coatings consist of a metallic bond coat, a composite layer (metal and alumina), a graded metal-alumina layer, another composite layer (metal and alumina), another mixed ceramic layer (alumina and zirconia), a full stabilized zirconia layer, another mixed ceramic layer (zirconia and alumina), and finally, a top ceramic layer (partially stabilized zirconia). This mixed structure coating can reduce thermal stresses between metals and ceramics related to the thermal expansion coefficient mismatch and lower cracking, thereby improving spalling resistance of the coating.

Schmitt-Thomas and Dietl (Ref 7) have studied the properties of a TBC consisting of a conventional metallic bond coat (NiCrAlY), a diffusion layer of alumina (2 to 5 μm thick), and a topcoat of partially stabilized $ZrO_2$. The diffusion layer was applied by physical vapor deposition (PVD). According to the results, the diffusion layer of alumina minimizes the bond coat oxidation and improves the adhesion strength of the ceramic layer. Cosack et al. (Ref 3) reported a decrease of residual stress at the ceramic-metallic interface obtained by cooling the substrate between 35 and 70 °C during spraying using atmosphere and temperature controlled spraying (ATCS).

In the present work, a new type of graded metal-ceramic coating is developed. The bond coat is a premixed metal-ceramic layer. Parameters are fixed during spraying for all the specimens. The number of layers and thicknesses were varied.

**C.R.C. Lima,** Methodist University of Piracicaba, S.Paulo, Brazil; and **R.-E. Trevisan,** State University of Campinas, S.Paulo, Brazil.

**Table 1 General characteristics of Inconel 718**

| | | | After aging | | | | |
|---|---|---|---|---|---|---|---|
| Hardness | Solution treating | Aging | Tensile strength, MPa | Yield point, MPa | Elongation, % | Area reduction, % | Charpy V -18 °C, J |
| 25 HRC, solution treated | 1010 °C/1.5 h/water | 790 °C/6 h/air | 1206 | 840 | 20.2 | 30 | 64 |

**Table 2 Chemical analysis of Inconel 718**

| Element | Composition, wt % |
|---|---|
| C | 0.03 |
| Si | 0.07 |
| Cr | 17.76 |
| Mo | 3.05 |
| Ni | bal. |
| Ti | 1.07 |
| Nb | 5.12 |
| Al | 0.57 |
| Fe | 18.8 |

**Table 3 Characteristics of metallic powder**

| Typical composition | Typical particle size | Melting point |
|---|---|---|
| 6% aluminum<br>94% Ni-Cr alloy | -120 to +325 mesh<br>(-120 to +45 μm) | 660 °C (1215 °F),<br>Al constituent |

**Table 4 Characteristics of ceramic powder**

| Typical composition | Typical particle size | Melting point |
|---|---|---|
| 92% $ZrO_2$<br>8% $Y_2O_3$ | -200 to +325 mesh<br>(-75 to +45 μm) | 2480 °C<br>(4500 °F) |

**Table 5 Variations proposed in the experiments**

| Variables | Options | | |
|---|---|---|---|
| Bond coat | 100 wt% metallic | 50 wt% metallic/50 wt% ceramic | 25 wt% metallic/75 wt% ceramic |
| No. of layers | 2 | 3 | 4 |
| Total thickness, μm | 300 | 500 | 700 |

## 2. Materials and Experimental Procedure

Substrates used in this study consisted of Inconel 718 superalloy. The general characteristics and nominal composition of these materials are given in Tables 1 and 2, respectively.

The metallic powder is a Ni-Cr-Al alloy, which undergoes an exothermic reaction during spraying. The metallic powder characteristics are given in Table 3. The ceramic powder is a spherical $ZrO_2$, partially stabilized with 8% $Y_2O_3$. The ceramic powder characteristics are given in Table 4.

The metallic and ceramic powders were chosen for compatible particle size, in the range of -120 to +45 μm for the metallic powder and -75 to +45 μm for the ceramic powder. This is an important characteristic for powder mixing homogeneity and for maintenance of this condition during thermal spraying.

The proposed system for the coatings is metal (M) and ceramic (C) powder graduation, by weight, at the intermediate coating layers without a conventional metallic bond coat, as shown in Fig. 1.

Thus, between the metallic substrate and the ceramic topcoat, mixed metal-ceramic layers were deposited. Graduation parameters for the coatings were determined according to Table 5, in keeping with the goal of the experiments and trying to establish a mutual relationship between the proposed and duplex systems. Each type of bond coat was tested for the three conditions of thickness and the number of layers in Table 5. The number of layers refers to the quantity of different schedules of metal-ceramic gradation. A layer is composed of sequential passes with the same metal-ceramic mixture. Deposition parameters used for plasma-spraying are summarized in Table 6.

Test specimens (ϕ 25 by 25 mm) were grit blasted prior to spraying. The bond strength measurements were performed in accordance with the ANSI-ASTM-C633-79 standard (Ref 8). The adhesive bonding agent used was a two-part mix cured at room temperature, epoxy-based, 3M-DP-460 (3M of Brazil). The nominal shearing strength of the adhesive is 31 MPa (4500 psi).

Metallographic specimens were observed in a metallographic test stand by Carl Zeiss, NEOPHOT-32. The microstructure and defect structure of the coatings were determined. Thickness measurements and cross section micrographs were performed. Surface morphology and microstructure were also observed by a scanning electron microscope, JEOL-JXA-840-A (JEOL). Energy-dispersive analysis x-ray (EDAX) was used to determine the concentration profile of the metallic and ceramic elements. Normal image and x-ray image micrographs of the top and cross section of the coatings were made. Distribution and the degree of metal-ceramic mixing were also observed.

## 3. Results and Discussion

### 3.1 *Adhesion Tests*

Results of the adhesion tests are given in Tables 7 to 9 for the 25 wt% metallic to 75 wt% ceramic (25-75), 50 wt% metallic to 50 wt% ceramic (50-50), and 100 wt% metallic (100-0) bond coat series, respectively. The thickness and number of layers of each test specimen are also included.

The fracture mode in the test may be adhesive (when occurring at the bond coat-substrate interface) or cohesive (when occurring within the coat). Failure in the bonding agent (within the adhesive) is not considered an effective result. Thus, the results determine the best cermet bond coat. However, according to Mittal (Ref 9), the measured adhesion value, obtained by dividing the failure load by the testing area (cross-sectional area) is the value of practical adhesion and not basic adhesion, which is

**Table 6 Deposition parameters for the coating deposition**

| | |
|---|---|
| Arc voltage, V | 60 to 70 |
| Arc current, A | 500 |
| Arc gas | argon-hydrogen |
| Ar flow rate, l/min | 80 |
| $H_2$ flow rate, l/min | 15 |
| Spray distance, mm | 80 |
| Deposition rate, Kg/h | 1.1 |
| Ar carrier gas flow rate, l/min | 37 |

**Table 7 Adhesion of specimens with 25 wt % metallic-75 wt % ceramic bond coat**

| Test specimen | Thickness, μm | No. of layers | Adhesion, MPa |
|---|---|---|---|
| cp 09 | 70 | 1 | 19.5 |
| cp 12 | 300 | 4 | 14.0 |
| cp 16 | 150 | 1 | 31.3 |
| cp 18 | 500 | 3 | 16.8 |
| cp 22 | 350 | 1 | 12.7 |
| cp 23 | 700 | 2 | 11.7 |

**Table 8 Adhesion of specimens with 50 wt % metallic-50 wt % ceramic bond coat**

| Test specimen | Thickness, μm | No. of layers | Adhesion, MPa |
|---|---|---|---|
| cp 01 | 200 | 1 | 20.8 |
| cp 04 | 700 | 4 | 8.8 |
| cp 19 | 100 | 1 | 12.5 |
| cp 21 | 300 | 3 | 13.5 |
| cp 24 | 250 | 1 | 17.9 |
| cp 25 | 500 | 2 | 19.4 |

**Table 9 Adhesion of specimens with 100 wt % metallic bond coat**

| Test specimen | Thickness, μm | No. of layers | Adhesion, MPa |
|---|---|---|---|
| cp 05 | 125 | 1 | 33.8 |
| cp 08 | 500 | 4 | 16.6 |
| cp 13 | 250 | 1 | 18.2 |
| cp 15 | 700 | 3 | 30.4 |
| cp 26 | 150 | 1 | 38.7 |
| cp 27 | 300 | 2 | 36.1 |

strictly an interfacial property and depends exclusively on the surface characteristics of adhering phases. Steffens et al. (Ref 10) indicate that basic adhesion may be evaluated by the degree of coverage of the substrate with powder particles after testing the bonding strength. Thus, the number of bonded particles on the substrate is also an indication of the bonding quality.

The variations in adhesion with the coating thickness (Tables 7 to 9) are compared in Fig. 2 for the different bond coats. As shown in Fig. 2, coatings with a metallic bond coat (100-0) have the greatest adhesion values, regardless of thickness. Exceptions were coatings 300 and 550 μm thick, which fractured at the adhesive and within the coating (second to third layer), respectively.

Variation of adhesion with the number of layers (Tables 7 to 9) is compared in Fig. 3. Adhesion values for one-layer coatings are the intermediate values for each table.

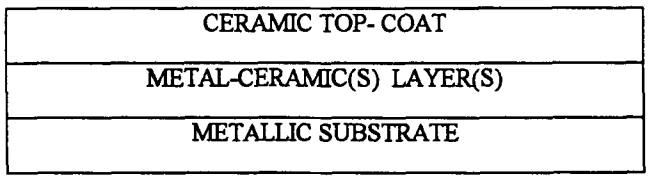


**Fig. 1** Typical structure of proposed graded TBC

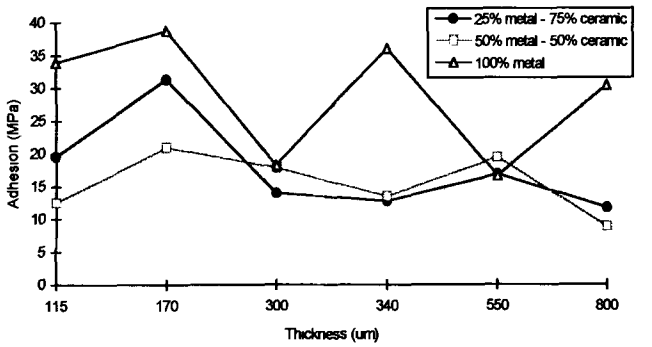


**Fig. 2** Variation of adhesion with the coating thickness

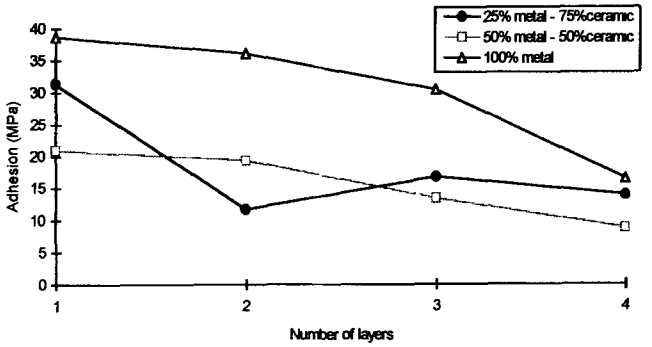


**Fig. 3** Variation of adhesion with the number of coating layers

In Fig. 3, a tendency of lower adhesion with an increase in layers can be observed. This tendency is not clear with increasing thickness (Fig. 3) but has been confirmed by other works (Ref 11). The value of the bond coat (25-75), with two layers in Fig. 4, does not follow the trend indicated by the thicker coating (700 μm). According to the experimental design, the increase in number of layers indicates that there was a greater interruption time for the subsequent spraying of layers with different metal-ceramic compositions to permit powder exchange and dust cleaning of the entire spraying system. The use of dual feeder and similar arrangements can solve this problem in practical applications. The increase in number of layers in Fig. 3 does not necessarily correspond to an increase of coating thickness.

Shaw and German (Ref 12), in a study of simultaneous spraying of metallic and ceramic powders (nickel and $Al_2O_3$), found that particles in the range of 0 to 50 μm segregate during plasma-spraying when the powder injection is normal to the jet axis, based on relative injection velocity, size, and density. As the distance increases from the point of injection, the coating structure

becomes metal rich because the density and radial inertia of the metal (nickel) particles are higher than similarly sized ceramic particles ($Al_2O_3$). These ceramic particles remain concentrated at the plasma jet center.

Sexsmith and Troczynski (Ref 13), in a similar study of plasma spraying of ceramic powders, aided by Monte Carlo simulation, found that lower adhesion occurs at the coating profile periphery, which indicates higher adhesion at the center and lower adhesion at the rim of a particular profile. The relationship of these results to this investigation follows. For coatings with a mixed 25-75 bond coat, the lower adhesion value (11.7 MPa) occurs for a two-layer 700 μm thick coating. The particle classification effects, in addition to the lower adhesion at the ceramic deposit periphery, affected the average value of adhesion because many passes were applied, and there was a gap between first and second layer application. This allowed cooling of the substrate and the first applied layer (thick layer) before spraying of the second layer. Residual thermal stresses were produced, and the summation of the various individual coating profiles resulted in a lower adhesion coating. This test specimen failed in a cohesive manner. The higher adhesion value for this group (31.3 MPa) is relative to the one-layer 150 μm thick coating. Thus, particle segregation and radial distribution effects did not have a significant influence on the adhesion values because there were not many overlapping individual patterns.

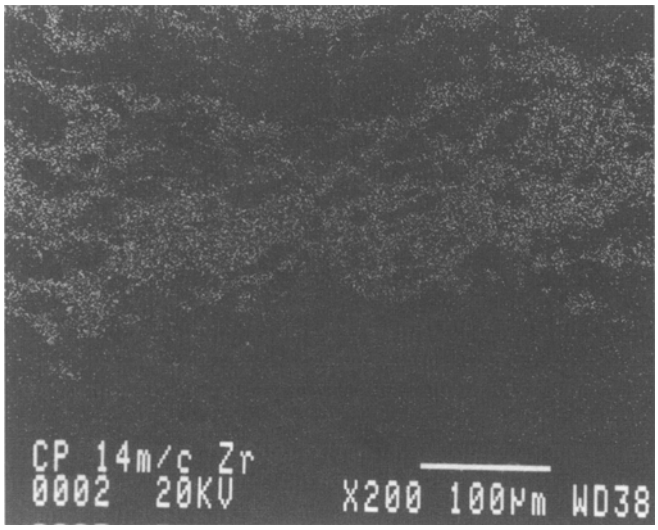


**Fig. 4** Map distribution of zirconium ($ZrO_2$ component) graded metal-ceramic coating x-ray image micrograph

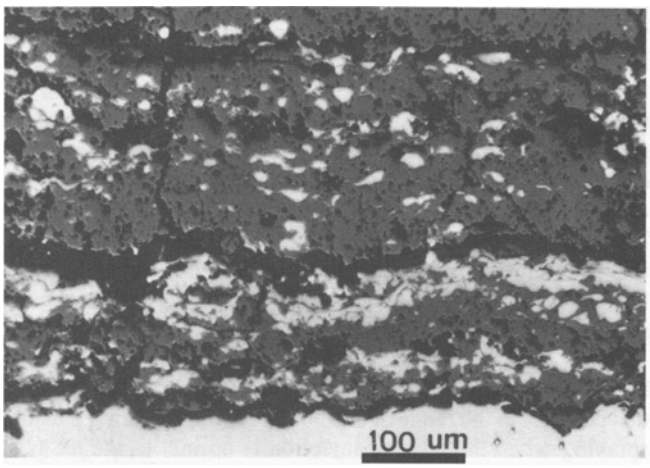


**Fig. 5** Optical micrograph of the cross section of a mixed metal-ceramic coating

For the coatings with mixed 50-50 bond coat, the lower adhesion value (8.82 MPa) occurs for the four-layer 700 μm thick coating. The one-layer 200 μm thick coating exhibits a higher adhesion value (20.8 MPa).

The lower adhesion value (16.6 MPa) for the coatings with a conventional metallic bond-coat (100-0) occurs for the four-layer 500 μm thick coating. The one-layer 150 μm thick coating exhibits a higher value (38.7 MPa). Accordingly, the increase in thickness and, concomitantly, the increase in the number of layers is detrimental to the adhesion.

For comparison purposes, powder manufacturers have established the following adhesion values for reference: (a) metallic powder is 27.6 MPa on series 300 stainless steel substrate with a

**Table 10 EDAX metal-ceramic composition in cross section analysis**

| Test specimen No. | Basic M-C composition, wt% | EDAX M-C composition, wt% | Variation, % |
|---|---|---|---|
| cp 09 | 25 - 75 | 4.9 - 95.1 | 20.1 |
| cp 12 | 13.5 - 86.5 | 9.2 - 90.8 | 4.3 |
| cp 16 | 25 - 75 | 15.2 - 84.8 | 9.8 |
| cp 18 | 10.5 - 89.5 | 2.3 - 97.7 | 8.2 |
| cp 22 | 25 - 75 | 32.3 - 67.7 | 7.3 |
| cp 23 | 12.5 - 87.5 | 16.8 - 83.2 | 4.3 |
| cp 01 | 50 - 50 | 56.8 - 43.2 | 6.8 |
| cp 04 | 23.5 - 76.5 | 36.3 - 63.7 | 12.8 |
| cp 19 | 50 - 50 | 45.2 - 54.8 | 4.8 |
| cp 21 | 25 - 75 | 33.4 - 66.6 | 8.4 |
| cp 24 | 50 - 50 | 17.9 - 82.1 | 32.1 |
| cp 25 | 25 - 75 | 23.9 - 76.1 | 1.1 |
| cp 05 | 100 - 0 | 100 - 0 | 0 |
| cp 08 | 56.2 - 43.8 | 34.9 - 65.1 | 21.3 |
| cp 13 | 100 - 0 | 100 - 0 | 0 |
| cp 15 | 53.5 - 46.5 | 40 - 59.9 | 13.4 |
| cp 26 | 100 - 0 | 100 - 0 | 0 |
| cp 27 | 50 - 50 | 34.9 - 65.1 | 15.1 |

**Table 11 EDAX metal-ceramic composition in top view analysis**

| Test specimen No. | Basic M-C composition, wt% | EDAX M-C composition, wt% | Variation, % |
|---|---|---|---|
| cp 09 | 25 - 75 | 12.9 - 87.1 | 12.1 |
| cp 10 | 20 - 80 | 36.7 - 63.3 | 16.7 |
| cp 11 | 10 - 90 | 0.2 - 99.8 | 9.8 |
| cp 17 | 10 - 90 | 2 - 98 | 8.0 |
| cp 22 | 25 - 75 | 12.5 - 87.5 | 12.5 |
| cp 23 | 0 - 100 | 4.8 - 95.22 | 4.8 |
| cp 19 | 50 - 50 | 25.3 - 74.7 | 24.7 |
| cp 20 | 25 - 75 | 22.6 - 77.4 | 9.6 |
| cp 21 | 0 - 100 | 6.9 - 93.1 | 6.9 |
| cp 05 | 100 - 0 | 100 - 0 | 0 |
| cp 06 | 75 - 25 | 78.3 - 21.7 | 3.3 |
| cp 07 | 50 - 50 | 74.1 - 25.4 | 24.6 |
| cp 08 | 0 - 100 | 0 - 100 | 0 |
| cp 13 | 100 - 0 | 100 - 0 | 0 |
| cp 27 | 0 - 100 | 0.6 - 99.4 | 0.6 |

spray distance of 125 to 150 mm (5 to 6 in.) and (b) ceramic powder is 21 MPa on low carbon steel with a metallic bond coat and a spray distance of 64 mm (2.5 in.).

Meterns-Lecomte et al. (Ref 14) obtained adhesion values between 12 and 31 MPa to characterize a variety of yttria-stabilized zirconia powders applied on Hastelloy X substrates with a NiCrAlY bond coat. The same ASTM-C633-79 test was used to obtain the adhesive strength of the specimens. Therefore, adhesion results obtained for coatings with mixed metal-ceramic bond coats, as proposed in this investigation, are considered satisfactory. It is important to remember that the spray parameters were not changed during the experiments, and therefore, optimization of the spray conditions may lead to better results.

### 3.2 *Microstructure and Phase Analysis*

The efficiency of the as-sprayed mixed metal-ceramic deposit related to the mixture previously fed was verified by x-ray energy dispersive analysis (EDAX). Results are given in Tables 10 and 11 for cross section and top view analysis, respectively.

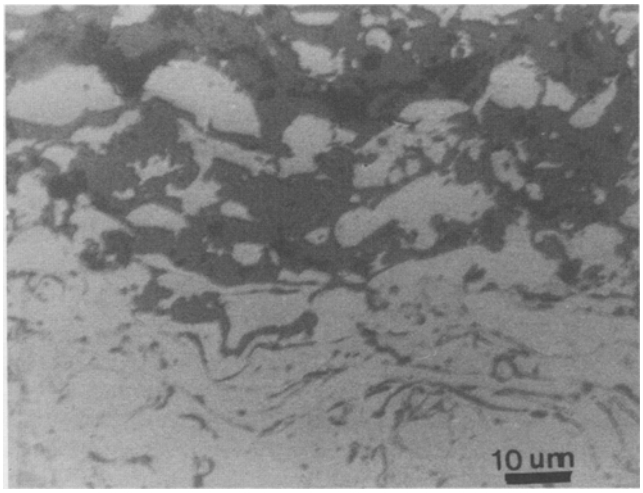


**Fig. 6** Cross section of a metallic/metal ceramic interface

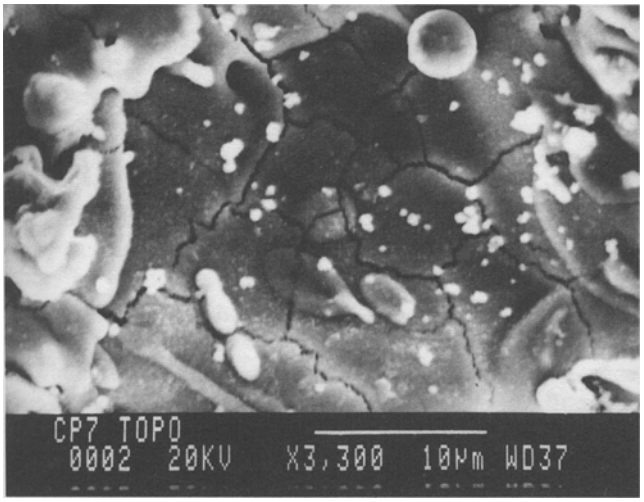


**Fig. 8** Microcracks on a ceramic fully molten region

Tables 10 and 11 show agreement with regard to mixture composition. The average variation for metal-ceramic phase composition is 9.8%. Figure 4 shows an x-ray image of zirconium for the cross section of a coating composed of a metallic bond coat (100-0) and a second layer of mixed metal-ceramic coat (50-50).

Good homogeneity of metal-ceramic distribution is observed in the coating. This homogeneity can also be observed in Fig. 5, which is a representative coating composed of a 50-50 metal-ceramic bond coat, a 25-75 metal-ceramic layer, a 10-90 metal-ceramic layer, and a top ceramic layer (0-100). The light regions are metallic.

Figure 6 shows the interfaces of a metallic/metal-ceramic coating. The presence of cracks and pores is lower than at the interface of a metallic/ceramic coating.

Morphology of the coating was also observed by SEM. The mixed metal-ceramic coating shows regions of fully molten ce-

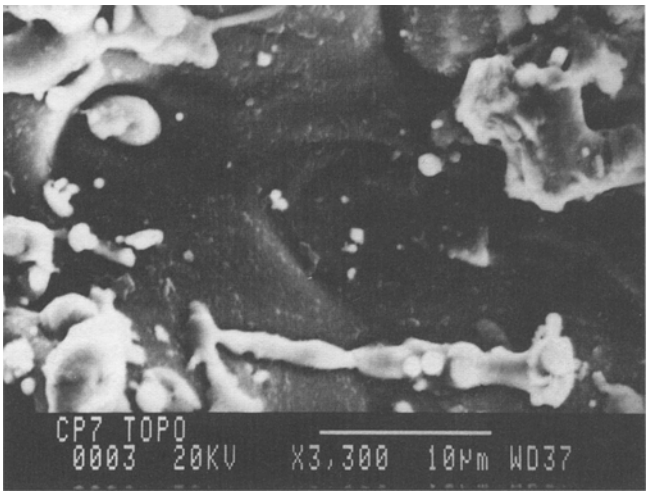


**Fig. 7** Top view of a metallic fully molten region

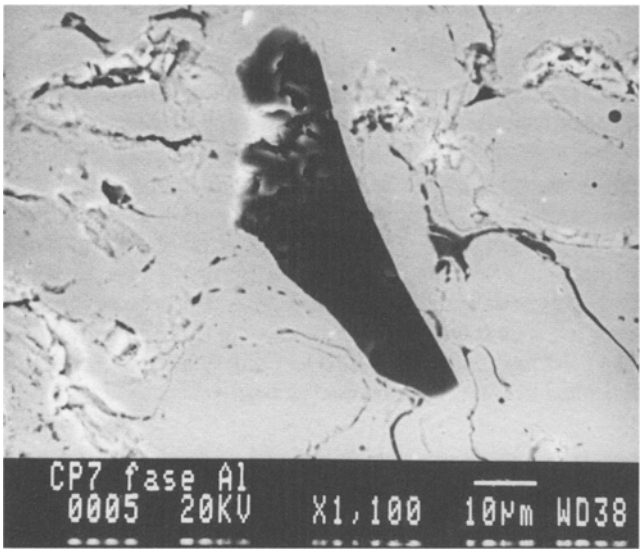


**Fig. 9** Cross section of a mixed metal-ceramic coating showing an aluminum-containing phase (dark area)

ramic particles and fully molten metallic particles. Ceramic regions, where particle wetting was higher, exhibited microcracks. These microcracks relieve thermal stresses during coating formation (Ref 15). Figures 7 and 8 show top views of these coating areas for a test specimen with a 50-50 metal-ceramic bond coat.

It was observed that coatings with a mixed 50-50 metal-ceramic structure have a tendency to present brittle precipitates of aluminum because of the spray procedure characteristics. Aluminum is a component of the metallic powder. Figure 9 shows an aluminum containing phase confirmed by x-ray diffraction. Generally, these phases lead to cracking of the coatings.

## 4. Conclusions

The following conclusions resulted from this work:

- The proposed method for metal-ceramic coatings spraying is encouraging, especially considering there was no optimization of process parameters, which were held constant during spraying.
- Increasing thickness tends to decrease coating adhesion regardless of the bond coat used.
- An increase in the number of layers tends to diminish coating adhesion, although overall thickness is not increased because of substrate cooling between the passes.
- The coatings produced with a 25-75 metal-ceramic powder gradation exhibit better phase stability, morphology, and microstructure than coatings with a 50-50 metal-ceramic gradation, which tend to exhibit aluminum-containing phases.
- Co-deposition of premixed metallic and ceramic powders forms coatings with a deposited metal-ceramic mixture similar to those previously established and homogeneously distributed.

### Acknowledgments

The authors would like to thank Rolls Royce Motors, Brazil, for their technical collaboration and to acknowledge the financial support of FAPESP, Brazil.

### References

1. K. Suganuma, Y. Myiamoto, and M. Koizumi, Joining of Ceramic and Metals, *Ann. Rev. Mater. Sci.*, Vol 18, 1988, p 47-73
2. M.L. Thorpe, Major Advances Noted in Thermal Spray Technology, *Adv. Mater. Process.*, Vol 1, Jan 1993, p 23-24
3. T. Cosack, L. Pawlowski, S. Schineiderbanger, and S. Sturlese, Thermal Barrier Coatings on Turbine Blades by Plasma Spraying With Improved Cooling, *J. Eng. Gas Turbines Power Trans. ASME,* (No. 116), 1991, p 272-276
4. M.R. Dorfman, B.A. Kushner, and A.J. Rotolico, *A Review of Thermal Barrier Coatings for Diesel Engines Applications,* Metco/Perkin Helmer Int. Com., 1991, p 19
5. H.L. Tsai and P.C. Tsai, Performance of Laser-Glazed Plasma Sprayed ($ZrO_2$ -12wt%$Y_2O_3$)/(Ni-22wt%Cr-10wt%Al-1wt%Y) Thermal Barrier Coatings in Cyclic Oxidation Tests, *Surf. Coat. Technol.*, Vol 71, 1995, p 53-59
6. J.T. Demasi-Marcin and D.K. Gupta, Protective Coatings in the Gas Turbine Engine, *Surf. Coat. Technol.*, Vol 68/69, 1994, p 1-9
7. K.G. Schmitt-Thomas and U. Dietl, Thermal Barrier Coatings with Improved Oxidation Resistance, *Surf. Coat. Technol.*, Vol 68/69, 1994, p 113-115
8. "Standard Method of Test for Adhesion or Cohesive Strength of Flame Sprayed Coatings," C633, *19th Annual Book of ASTM Standards,* Part 17, ASTM, 1979, p 636-642
9. K.L. Mittal, "Adhesion Measurement: Recent Progress, Unsolved Problems and Prospects," *ASTM Special Tech. Publications 640,* ASTM, 1978, p 5-17
10. H.D. Steffens, Z. Bablak, and W. Brandi, Thermal Barrier Coatings: Some Aspects of Properties Design, *Thermal Spray Coatings: Properties, Process and Applications,* T.F. Bernecki, Ed., ASM International, 1991, p 289-294
11. D.J. Greving, J.R. Shadley, and E.F. Rybicki, Effects of Coating Thickness and Residual Stresses on Bond Strength of C633-79 Thermal Spray Coating Test Specimen, *Thermal Spray Industrial Applications,* C.C. Berndt and S. Sampath, Ed., ASM International, 1994, p 639-645
12. K.G. Shaw and R.M. German, Particle Classification Effects During Plasma Spraying, *Thermal Spray Industrial Applications,* C.C. Berndt and S. Sampath, Ed., ASM International, 1994, p 399-404
13. M. Sexsmith and T. Troczynski, The Variations in Coating Properties Across a Spray Pattern, *Thermal Spray Industrial Applications,* C.C. Berndt and S. Sampath, Ed., ASM International, 1994, p 751-757
14. C. Meterns-Lecomte, D. Muck, and J. Garcia, Characterization of a New Aerospace Thermal Barrier Coating, *Thermal Spray Industrial Applications,* C.C. Berndt and S. Sampath, Ed., ASM International, 1994, p 61-65
15. W.J. Brindley and R.A. Miller, TBCs for Better Engine Efficiency, *Adv. Mater. Process.*, Vol 136 (No. 2), 1989, p 29-33